



Tailoring amide *N*-substitution to direct liquid crystallinity in benzanilide-based dimers

Grant J. Strachan^{*}, Amerigo Zattarin, John M.D. Storey, Corrie T. Imrie

Department of Chemistry, School of Natural and Computing Sciences, University of Aberdeen, Meston Building, Aberdeen AB24 3UE, UK

ARTICLE INFO

Keywords:

Benzanilide
Conformational analysis
Liquid crystals
Nematic phase
NMR spectroscopy

ABSTRACT

The design of liquid crystalline dimers containing tertiary benzanilide groups has proved challenging due to their strong preference for the *E* amide conformation. In this work we have investigated the effect of different *N*-substituents on the amide conformation of model benzanilide monomers and found this had effectively no effect on conformation. Based on this observation, we investigated the effect of introducing large, flexible decyl chains at the amide nitrogen and compare their properties to the corresponding benzanilide-based dimers with lateral methyl substituents. The introduction of the decyl chain decreases the melting temperatures, and the tendency to crystallise, promoting glassy behaviour. This allows for nematic behaviour to be seen to much lower temperatures.

1. Introduction

A conventional low molar mass liquid crystal typically consists of molecules containing a single semi-rigid core attached to which are one or two terminal chains. In essence, the interactions between the cores account for the observation of liquid crystallinity whereas the alkyl chain is used to modify the melting point and phase behaviour. The core, referred to as the mesogenic unit, normally comprises of phenyl rings linked through short unsaturated linkages, most commonly ester, imine or azo groups. Surprisingly the amide group does not feature amongst these linkages although has been widely used in liquid crystal polymers.

The amide group is structurally similar to the ester group, which has been particularly widely used as a linking group joining two phenyl rings in mesogenic units, and the equivalent amide-linked structure is known as a benzanilide. Secondary (2°) benzanilides have a hydrogen atom attached to the amide nitrogen, while in tertiary (3°) benzanilides this is replaced with an additional substituent. Early studies of liquid crystals containing 2° benzanilides report relatively high melting points compared to equivalent ester-linked materials, and also note that intermolecular hydrogen bonding between amide groups promoted smectic behaviour.[1] Although the generally high transition temperatures of such benzanilide-based materials may be undesirable, it has been shown that suitable structural modifications can give materials that form liquid crystal phases below 100 °C.[2] The change from 2° to 3° (*N*-methyl) benzanilide structures has been reported to lead to the

loss of liquid crystallinity.[3].

We have shown recently that this loss of liquid crystallinity for dimers containing tertiary benzanilides is due to a change in the amide conformational preference from the *Z* to the *E* form, (Fig. 1), which destroys the anisometric molecular structure required for the observation of liquid crystalline behaviour.[4] Our previous study showed that suitable modifications to the dimer structure promoted the formation of nematic phases, however, the temperature range of liquid crystalline behaviour was very limited compared to the liquid crystalline properties of the analogous 2° benzanilides.[5] This raised the question as to whether it is possible to control the amide conformational preferences by using different *N*-substituents. In addition, since it was found that monotropic nematic phases were formed for some 3° benzanilide-based dimers, could suppressing crystallinity through the inclusion of flexible substituents on the amide nitrogen allow for an increased diversity of liquid crystalline behaviour?

In the first part of this study, we have prepared a range of benzanilide-based monomers, with a lateral methyl substituent *ortho* to the amide group. We refer to these molecules as monomers as they contain a single rigid moiety whereas a dimer contains two separated by a flexible spacer.[6] We investigate the effects that changing the size of the nitrogen substituent has on the amide rotational barrier using methyl, ethyl, and allyl *N*-substituents (Fig. 2). In the second part, we have applied these results to design a series of new mesogenic materials based on laterally substituted benzanilide dimers (Fig. 3) and report

^{*} Corresponding author at: School of Chemistry, Trinity Biomedical Sciences Institute, Trinity College Dublin, Dublin 2, Ireland.

E-mail address: gj.strachan@outlook.com (G.J. Strachan).

<https://doi.org/10.1016/j.molliq.2023.122160>

Received 21 December 2022; Received in revised form 8 May 2023; Accepted 19 May 2023

Available online 22 May 2023

0167-7322/© 2023 The Authors. Published by Elsevier B.V. This is an open access article under the CC BY license (<http://creativecommons.org/licenses/by/4.0/>).

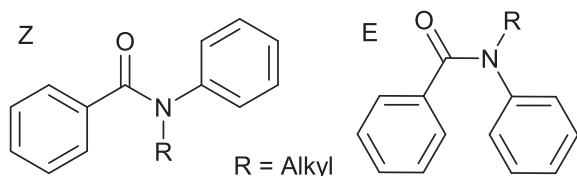


Fig. 1. The *Z* and *E* conformations of tertiary benzanilides.

their rotational barriers and liquid crystalline properties.

2. Experimental

The syntheses of the target molecules shown in Figs. 1 and 2 were carried out according to literature methods, and full experimental details and structural characterisation data are given in the ESI.

The transitional behaviour of the materials was studied using differential scanning calorimetry (DSC) with a Mettler Toledo DSC3 differential scanning calorimeter equipped with a TSO 801RO sample robot and calibrated with indium and zinc standards. The heating and cooling rates were $10\text{ }^{\circ}\text{C min}^{-1}$ and the transition temperatures and their associated enthalpy changes were extracted from heating traces unless otherwise noted. Polarised optical microscopy (POM) was used to identify the liquid crystal phases using an Olympus BH2 polarising optical microscope equipped with a Linkam TMS 92 hot stage.

Variable temperature ^1H NMR experiments were carried out on a Bruker Avance III HD 400 MHz spectrometer with a cryoprobe and VT unit. Lineshape analysis was performed using the DNMR module in the Bruker TOPSPIN package. 2D EXSY measurements were carried out on a Bruker Avance III HD 400 MHz spectrometer and processed using the

Mestrelab EXSYCalc program.

3. Results and discussion

3.1. Influence of the *N*-substituent on amide conformation

In the first part of this work, we prepared a range of 3° benzanilide-based monomers (Fig. 1) as model compounds to establish the effect that varying the size of the *N*-substituent has on the *E*:*Z* conformer ratio. For each *N*-substituent, a set of monomers with differing terminal chain lengths have been studied. For all the *N*-substituents (methyl, ethyl, and allyl), the ^1H NMR spectrum of each compound in solution shows the presence of a minor conformer, as previously reported for similar 3° amide-based dimers.[4] For the *N*-Me-substituted benzanilides, the minor conformer gives rise to minor side peaks adjacent to the methyl signals, in approximately a 1:9 ratio, as well as a set of minor peaks in the aromatic region (Fig. 4).

Variable temperature NMR spectroscopic measurements show that the minor and major peaks broaden and coalesce on heating, which indicates that they must be associated with rotational conformers separated by a rotational energy barrier. The stacked VT NMR spectra of compound **1b** (Fig. 5) is given as a representative example. The spectra of all the compounds show very similar behaviour on heating, and in each, the major and minor peaks coalesce at $50\text{ }^{\circ}\text{C}$. This suggests that the rotational energy barriers in these compounds are approximately the same and similar to those previously reported.[4,5].

Lineshape analysis of the NMR spectra was carried out using the TOPSPIN program to obtain the value of the rotational rate constant at each temperature. These can then be used to calculate the energy barrier using a standard Eyring plot shown for compound **1b** in Fig. 6. Using the

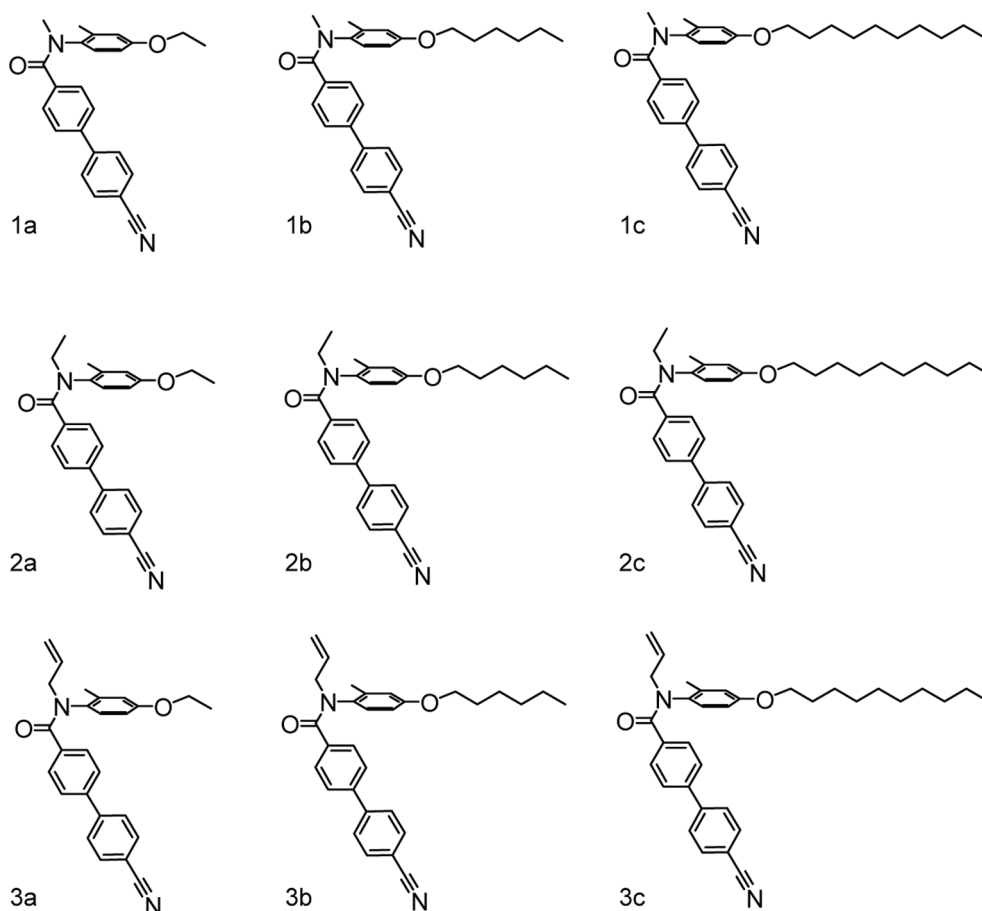


Fig. 2. The structures of the 3° benzanilide-based monomers.

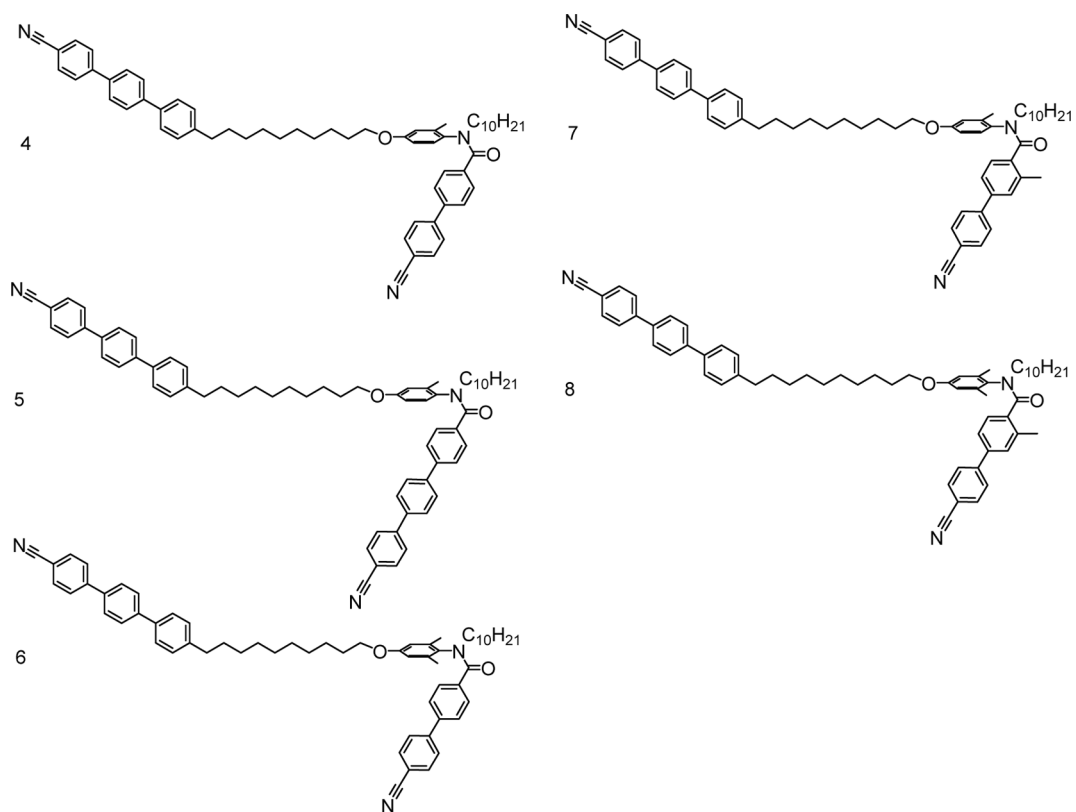


Fig. 3. The structures of the 3° benzamide-based dimers.

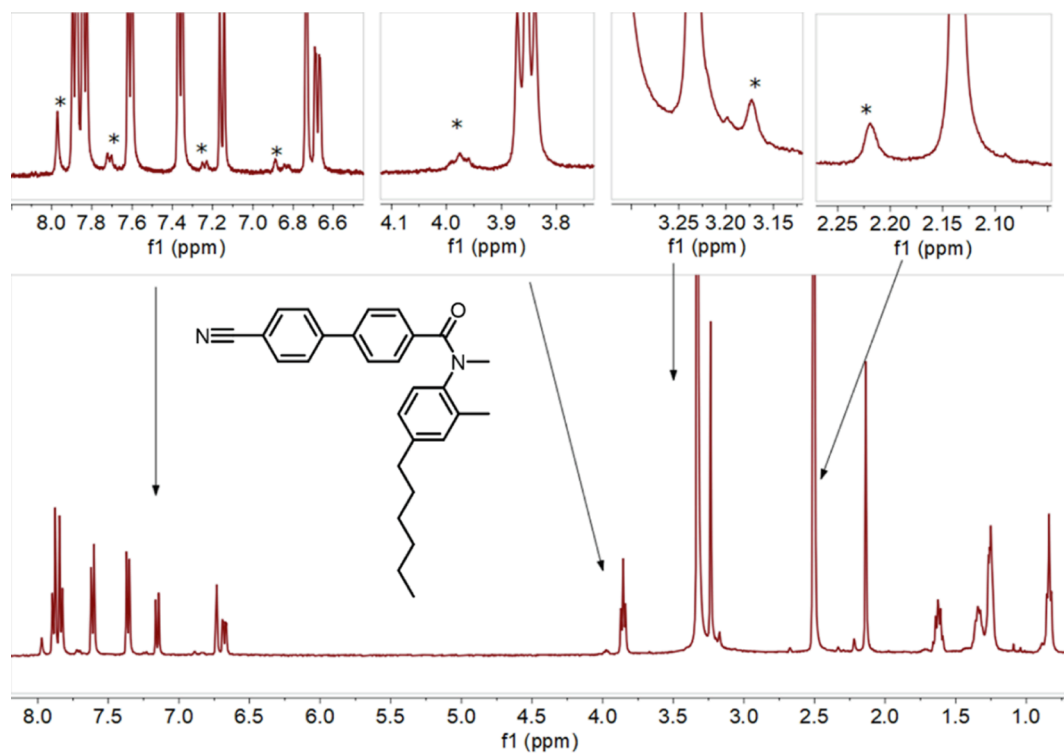


Fig. 4. ^1H NMR spectra of compound **1b** in $\text{DMSO}-d_6$. Inset regions show the minor peaks present at room temperature arising from the presence of a minor conformer.

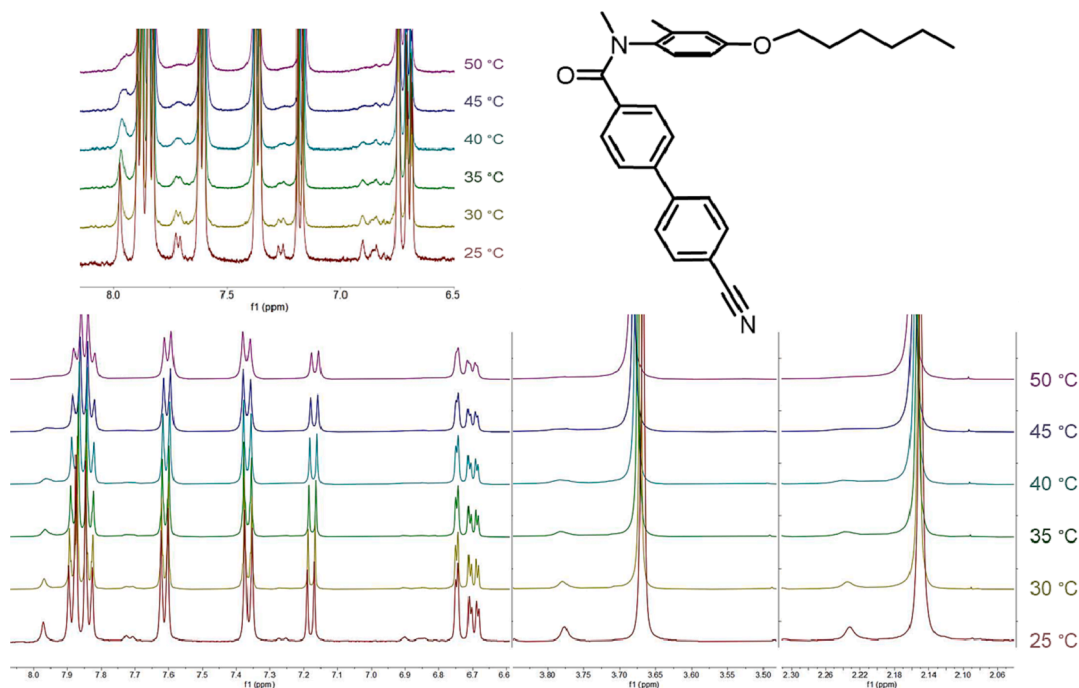


Fig. 5. Stacked VT ^1H NMR spectra of **1b** in $\text{DMSO-}d_6$ from 25 to 50 $^\circ\text{C}$.

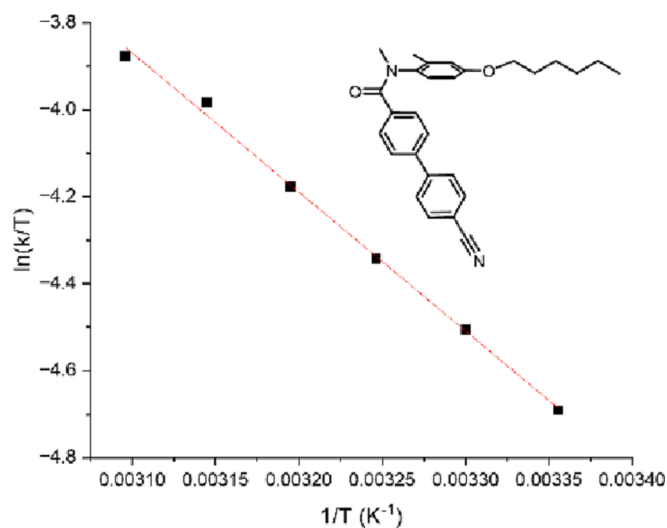


Fig. 6. Eyring plot of compound **1b** in $\text{DMSO-}d_6$ between 25 and 50 $^\circ\text{C}$.

Table 1

The rotational barriers of the 3° benzanilide-based monomers.

Compound	ΔG_{298}^\ddagger (kJ mol $^{-1}$)
1a	70.8 ± 1.2
1b	70.3 ± 0.84
1c	69.5 ± 0.84
2a	70.7 ± 0.84
2b	69.5 ± 1.3
2c	70.3 ± 1.7
3a	69.9 ± 1.3
3b	69.5 ± 0.84
3c	69.9 ± 1.3

equation:

$$\ln \frac{k}{T} = -\frac{\Delta H^\ddagger}{R} \cdot \frac{1}{T} + \ln \frac{k_B}{h} + \frac{\Delta S^\ddagger}{R}$$

In which ΔH^\ddagger is the enthalpy change associated with the rotation, ΔS^\ddagger is the associated entropy change, R is the gas constant, k_B is the Boltzmann constant and h is Planck's constant. From this, we can obtain the enthalpy and entropy associated with rotation, and hence the Gibbs energy barrier to rotation.[7] These rotational barriers are listed in Table 1, and the values for each compound are identical within experimental error. Eyring plots for all compounds are given in the SI.

Based on these results, we have established that the size of the N -substituent, within the scope of this study, has no discernible effect on the rotational barrier around the N -carbonyl bond in compounds with one methyl group *ortho* to the amide. Building on this observation, we incorporated large, flexible N -decyl substituents into a series of previously reported 3° benzanilide-based dimers containing N -methyl substituents that tended to exhibit monotropic nematic behaviour and showed a pronounced tendency to crystallise.[5] The structures of the new dimers are given in Fig. 2. Here we sought to exploit the design potential of varying the N -substituent, and the introduction of the large, flexible decyl chain was intended to suppress crystallisation and reveal further liquid crystal behaviour. This may initially appear counter-intuitive given that replacement of the compact methyl group by the large decyl chain will reduce the compound's structural anisotropy and hence presumably reduce the tendency to exhibit liquid crystalline behaviour. There are many examples of liquid crystals, however, with long lateral alkyl chains, and their liquid crystalline behaviour is accounted for by the ability of the flexible chain to adopt conformations in which it can lie along the molecular long axis.[8–13].

Fig. 7 shows the ^1H NMR spectra of the 3° benzanilide-based dimers containing an N -decyl substituent. The splitting patterns in the spectra, and the estimated proportions of E and Z amide conformers (based on the signals of the methyl substituent *ortho* to the nitrogen), are very close to those of the corresponding N -methyl substituted dimers reported previously.[5] (Table 2).

The signals associated with the N - CH_2 protons in the ^1H NMR spectra shows differences between the 3° benzanilide-based dimers (Fig. 8).

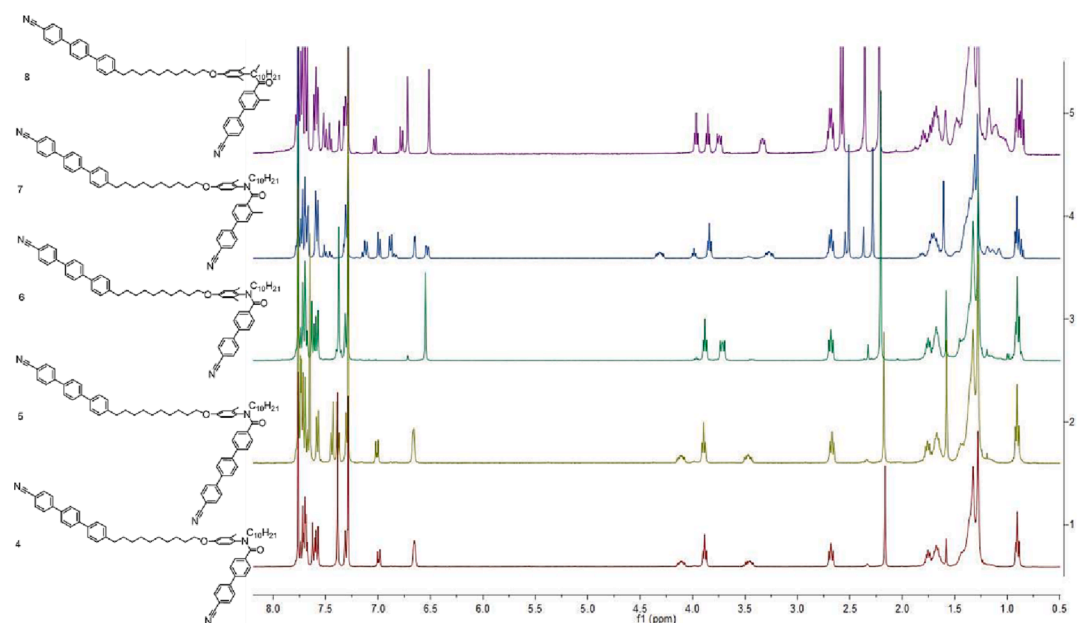


Fig. 7. The ^1H NMR spectra of the *N*-decyl substituted 3° benzanilide-based dimers.

Table 2

The *E*:*Z* ratio determined by ^1H NMR spectroscopy for the *N*-decyl substituted 3° benzanilide-based dimers. () Ratio on initial dissolution.

	<i>E</i> : <i>Z</i> (CDCl_3)	<i>E</i> : <i>Z</i> ($\text{DMSO}-d_6$)
4	17:1	12:1
5	18:1	11:1
6	16:1	10:1
7	4:1	2:1
8	1:1 (1:5)	1:2

Considering first dimers 4 and 5, both have a single *ortho* substituent on the anilide ring and differ only in having a cyanobiphenyl or cyanoterphenyl terminal group, respectively. The *N*- CH_2 signals in the ^1H NMR spectra of these compounds appear as diastereotopic multiplets due to restricted rotation around the nitrogen to aryl bond. In the symmetrically di-*ortho* substituted compound 6, the peak associated with the *N*- CH_2 group appears as a single multiplet, with an additional small peak corresponding to the *Z* amide conformer. In the asymmetrically di-substituted compound 7, the peak associated with the *N*- CH_2 group appears as two diastereotopic multiplets due to restricted rotation around the nitrogen to aryl bond as also seen in the spectra of 4 and 5.

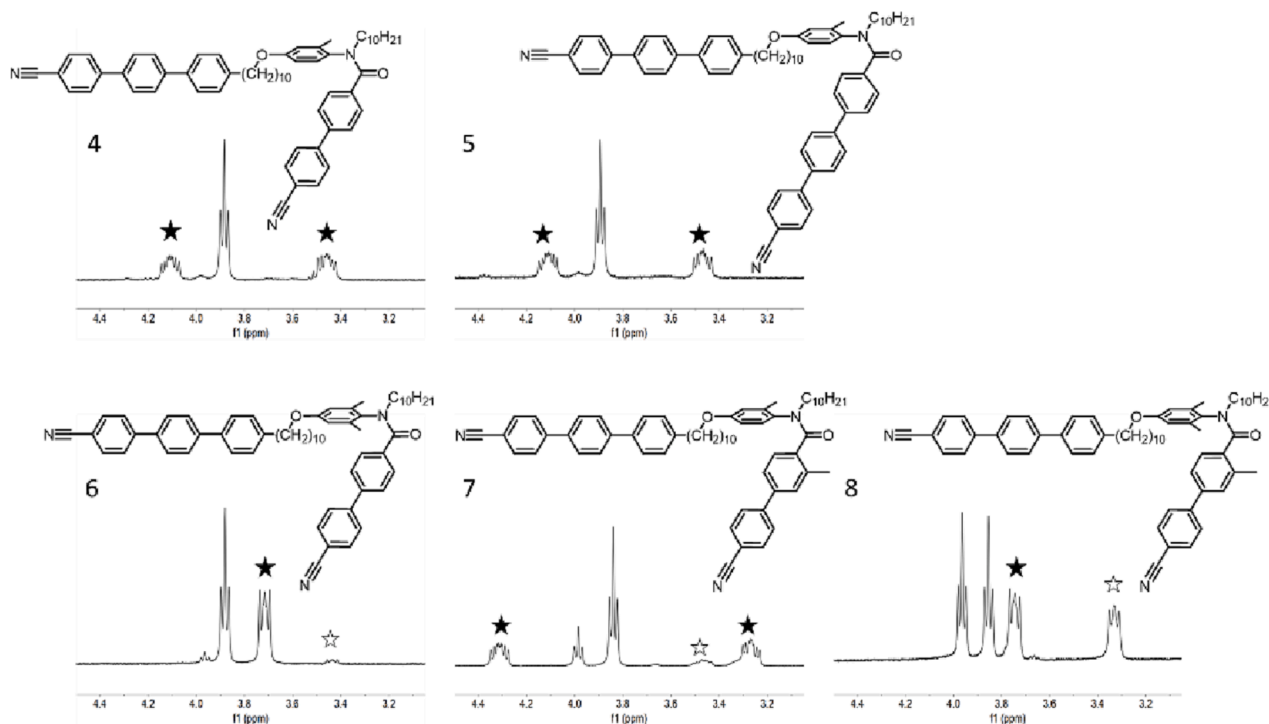


Fig. 8. The ^1H NMR peaks associated with the *N*- CH_2 protons in dimers 4–8. The signals for the *E* conformer are marked by *, and the *Z* conformer by *. The *Z* conformers of 4 and 5 are too weak to be seen.

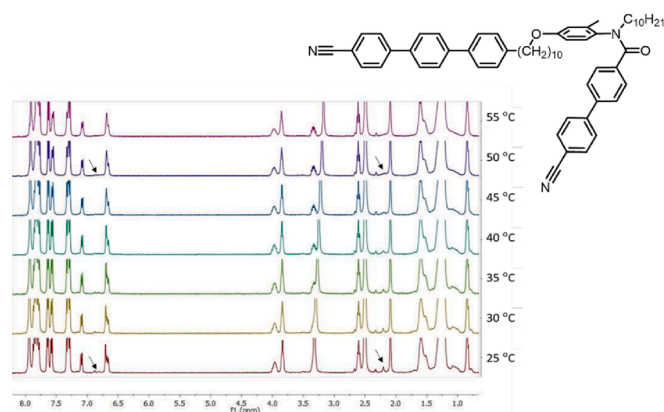


Fig. 9. VT ^1H NMR spectra of **4** in $\text{DMSO}-d_6$ from 25 to 55 $^\circ\text{C}$. Arrows indicate the peaks associated with the *Z* conformer.

The peak associated with the *N*- CH_2 group in the tri-*ortho* substituted compound **8** does not show diastereotopic splitting, as the anilide ring is symmetrically substituted, as seen also for compound **6**. Compound **8** appears to consist of an approximately 1:1 mix of *E*:*Z* isomers in CDCl_3 , and two signals are seen for the *N*- CH_2 protons.

3.2. Variable temperature (VT) ^1H NMR spectroscopic measurements of the amide *N*- $\text{C}(\text{O})$ rotational barrier

The VT ^1H NMR spectra for compound **4** are shown in Fig. 9, and it can be seen that the peaks associated with the *Z* and *E* conformers coalesce on heating.[4] In contrast, the diastereotopic signals associated with the *N*- CH_2 protons do not. This observation is consistent with the diastereotopicity arising from restricted rotation around the nitrogen-aryl bond, rather than the central amide *N*- $\text{C}(\text{O})$ bond. Whereas the

coalescence of the signals corresponding to the *E* and *Z* conformers of the compounds with a single *ortho* methyl substituent may be followed by VT NMR spectroscopy, the inclusion of additional methyl substituents *ortho* to the amide group leads to an increase in the rotational barrier around the *N*- $\text{C}(\text{O})$ bond, and as a result no coalescence is seen within the temperature range of the experiments. In consequence, alternative NMR spectroscopy-based approaches were used to determine the barrier to rotation in these dimers, and these are described in the following sections.

3.3. NMR measurements of the amide *N*- $\text{C}(\text{O})$ rotational barrier using 2D EXSY

The rotational barriers around the amide *N*- $\text{C}(\text{O})$ bond were determined for compounds **4** and **7** using 2D EXSY measurements in CDCl_3 and the details are given in Table 3 and Table 4, respectively. This approach calculates two rotational barriers, the first relating to the exchange signal between the *E* and *Z* NMR peaks and the second to the signal between the *Z* and *E* peaks. The average rotational barriers and their standard deviations for compound **4** are: $\Delta G^\ddagger_1 = 74.9 \pm 1.17 \text{ kJ mol}^{-1}$ and $\Delta G^\ddagger_2 = 66.4 \pm 0.57 \text{ kJ mol}^{-1}$. These energies are consistent with those measured for other tertiary benzanilides with a single *ortho* methyl substituent and thus, may be assumed as being representative of that for compound **5**.⁴ The symmetrically di-*ortho* substituted compound **6** showed no exchange signals, even at mixing times of 800 ms, and hence, this method could not be used to determine the rotational barrier for this compound. The absence of exchange signals indicates, however, that the rotational barrier for **6** must be significantly higher than that of **4**. The average rotational barriers and their standard deviations for compound **7** are: $\Delta G^\ddagger_1 = 81.8 \pm 1.76 \text{ kJ mol}^{-1}$ and $\Delta G^\ddagger_2 = 77.9 \pm 0.94 \text{ kJ mol}^{-1}$. These values are greater than those determined for the singly *ortho* substituted compound **4** and this is consistent with the increased steric bulk introduced by the second *ortho* methyl group on the carbonyl

Table 3
2D EXSY integrals, rate constants, and rotational barriers for compound **4** in CDCl_3 .

	τ_m / s	Integral				Rate constant / s^{-1}		Rotational barrier / kJ mol^{-1}	
		<i>EE</i>	<i>EZ</i>	<i>ZZ</i>	<i>ZE</i>	k_1	k_2	ΔG^\ddagger_1	ΔG^\ddagger_2
Ar- CH_3	0.005	20.41	•	1.00	•	•	•	•	•
	0.05	63.46	1.34	1.00	0.41	0.22	14.45	76.75	66.35
	0.1	98.25	2.71	1.00	2.32	0.48	11.40	74.80	66.94
	0.15	511.34	18.32	1.00	15.00	0.79	19.60	73.57	65.60
	0.2	1.30	0.06	0.01	0.05	0.46	11.17	74.91	66.99
	0.25	26.64	1.31	0.08	1.00	0.57	15.10	74.38	66.24

Table 4
2D EXSY integrals, rate constants, and rotational barriers for compound **7** in CDCl_3 .

	τ_m / s	Integral				Rate constant / s^{-1}		Rotational barrier / kJ mol^{-1}	
		<i>EE</i>	<i>EZ</i>	<i>ZZ</i>	<i>ZE</i>	k_1	k_2	ΔG^\ddagger_1	ΔG^\ddagger_2
Ar- CH_3	0.005	3.65		1.00					
	0.05	1358.66	2.66	387.28	1.00	0.01	0.14	83.54	77.84
	0.1	4.72	0.02	1.34	0.03	0.06	0.15	79.86	77.64
	0.15	510.20	1.50	141	1.00	0.01	0.07	83.73	79.52
	0.2	124.70	1.24	35.00	1.00	0.04	0.18	80.94	77.23
	0.25	90.40	1.09	25.18	1.00	0.04	0.18	80.71	77.29

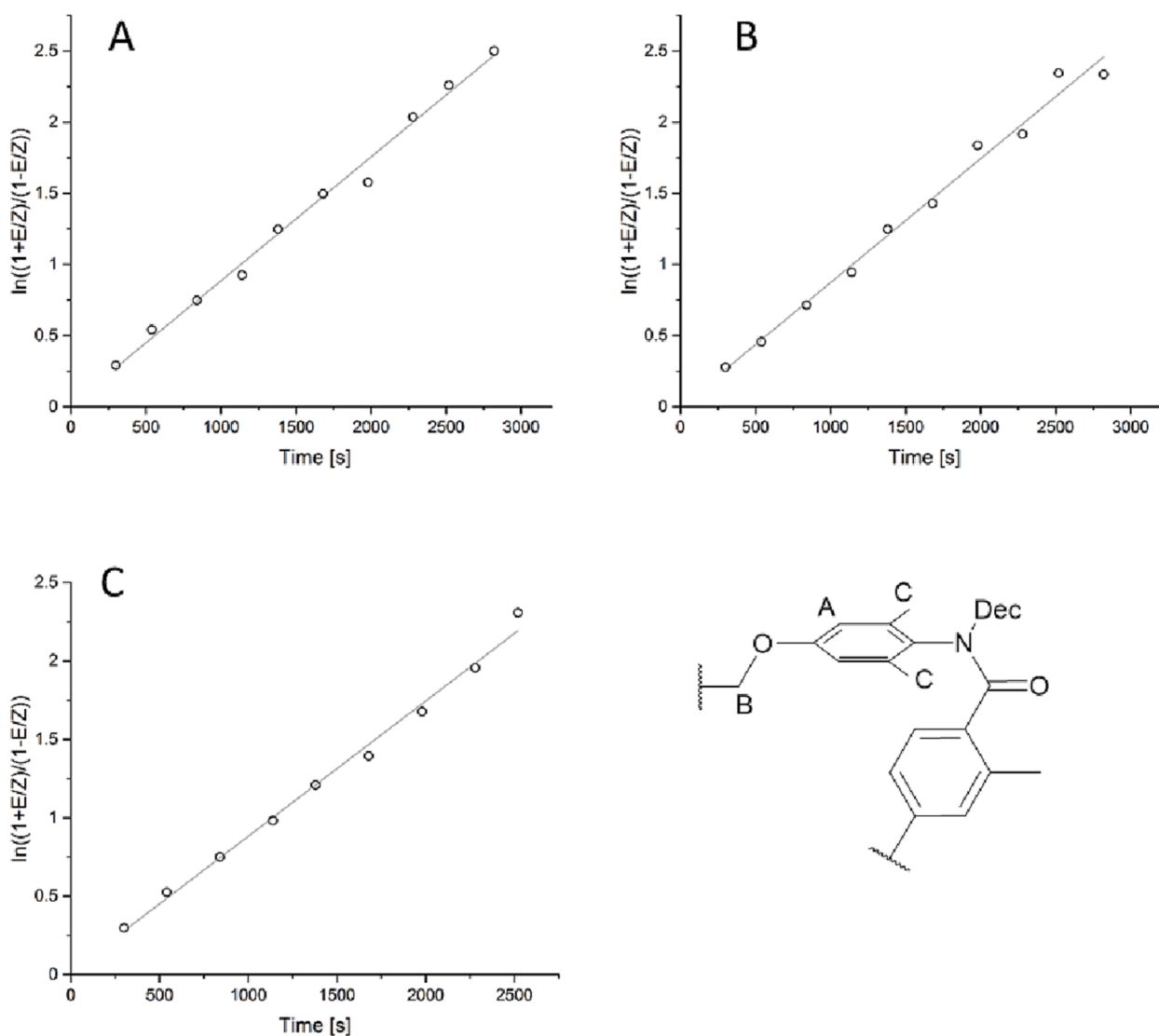


Fig. 10. Equilibration of the *E* and *Z* conformers of compound **8** measured by ^1H NMR spectroscopy in CDCl_3 for three different proton signals: the anilide protons (A), the first methylene group of the chain (B) and the anilide methyl signals (C).

Table 5

Linear fit and rotational constants for the equilibration of compound **8** in CDCl_3 .

Signal	Slope / s^{-1}	k / s^{-1}	ΔG^\ddagger / kJ mol $^{-1}$	R^2
Anilide protons (A)	8.707×10^{-4}	4.354×10^{-4}	92.1	0.992
O- CH_2 (B)	8.714×10^{-4}	4.357×10^{-4}	92.1	0.988
Anilide methyl groups (C)	8.615×10^{-4}	4.308×10^{-4}	92.2	0.993

ring of the benzanilide. Similar to the spectra recorded for **6**, an absence of exchange signals was also apparent for the tri-substituted compound **8**. This implies that having two *ortho* methyl substituents on the same ring greatly increases the barrier to rotation around the amide bond. This appears reasonable, as when the molecule has two *ortho* methyl substituents, there is no way to rotate the amide bond without rotating one of the methyl groups past the other ring; whereas in the singly *ortho* substituted compounds, the smaller hydrogen substituent can be rotated past the other ring.

The tri-substituted dimer **8** was isolated in the *Z* conformation by crystallisation, which then equilibrates on dissolution, and this is similar

Table 6

Transition temperatures and associated enthalpy and scaled entropy changes for the 3° benzanilide-based dimers (Fig. 2). † Denotes values taken from DSC cooling trace. *Glass transition.

	Reheat Melt / °C	Melt / °C	ΔH /kJ mol $^{-1}$	ΔS /R	N-I / °C	ΔH /kJ mol $^{-1}$	ΔS /R
4	52	118	15.7	4.8	56	0.72	0.26
5	36*	134	25.5	7.5	116	0.34	0.04
6	47	51	8.96	3.3	•	•	•
7	56	58	7.44	2.7	57†	•	•
8	36*	108	44.4	14	77	0.25	0.09

to the behaviour seen for the corresponding *N*-methylated analogue reported previously.⁵ This allows for the rotational barrier about the amide N-C(O) bond to be determined by following the rate of equilibration of the *E* and *Z* conformers using NMR spectroscopy (Fig. 10 and Table 5). The average rotational barrier and standard deviation for compound **8** is $\Delta G_{298}^\ddagger = 92.1 \pm 0.02$ kJ mol $^{-1}$. The rotational barrier for **8** is markedly higher than that of either the singly *ortho* substituted **4** or the di-substituted **7**, as would be expected for the more substituted compound.

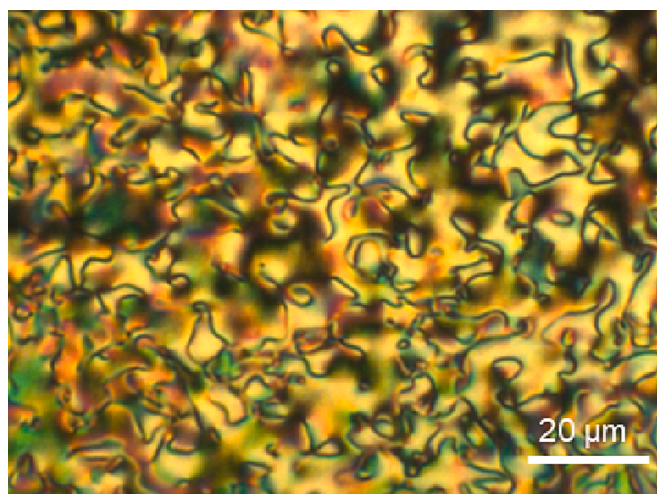


Fig. 11. Schlieren texture seen for **8** in the nematic phase at 45 °C.

3.4. Thermal properties of tertiary benzanilide-based dimers with an *N*-decyl group

The transition temperatures and associated enthalpy and scaled entropy changes for the 3° benzanilide-based dimers are listed in Table 6. **6** did not exhibit liquid crystalline behaviour whereas the other four dimers showed a monotropic nematic phase. This was identified on the

basis of the observation of schlieren textures containing two- and four-point defects and a representative example seen for **8** is shown in Fig. 11. The initial melting points for **4** and **5** obtained by crystallisation from a solvent were considerably higher than those measured on the second heating run (see Fig. 12). On cooling the nematic phase of compound **4** there was no clear change in texture but a marked increase in viscosity was apparent at 48°C corresponding to the exotherm seen in the DSC trace. The value of the entropy change associated with this transition strongly suggests the formation of a disordered or soft crystal. On reheating, this soft crystal phase melts into the nematic phase at 52 °C and subsequently clears into the isotropic phase at 56 °C. This is further confirmation that this lower temperature phase is a soft crystal phase. After storing the sample at room temperature for over a year, the sample does not form the original crystal phase, see Fig. 12. Instead, the aged sample appears to show a weak glass transition prior to the soft crystal – nematic transition, see inset Fig. 12. Vitrification of soft crystal phases is a well-known phenomenon, (see, for example ref 14). [14].

Compound **5** initially melts directly into the isotropic phase at 134 °C, and on cooling it enters the nematic phase at 115 °C, and forms a glass at 34 °C. On subsequent reheating, the glass transition occurs at 36 °C.

The value of T_{NI} for **5** is some 60 °C higher than that of **4**, and this reflects the exchange of a cyanobiphenyl unit in **4** for a cyanoterphenyl group in **5** and the associated increase in structural anisotropy accounts for the increase in T_{NI} . The symmetrically di-*ortho* substituted compound **6** does not show liquid crystal behaviour and crystallises at 46 °C. Compared to the singly *ortho* substituted **4** this suggests a reduction in T_{NI} of at least 10 °C. In contrast to this, the asymmetrically di-substituted

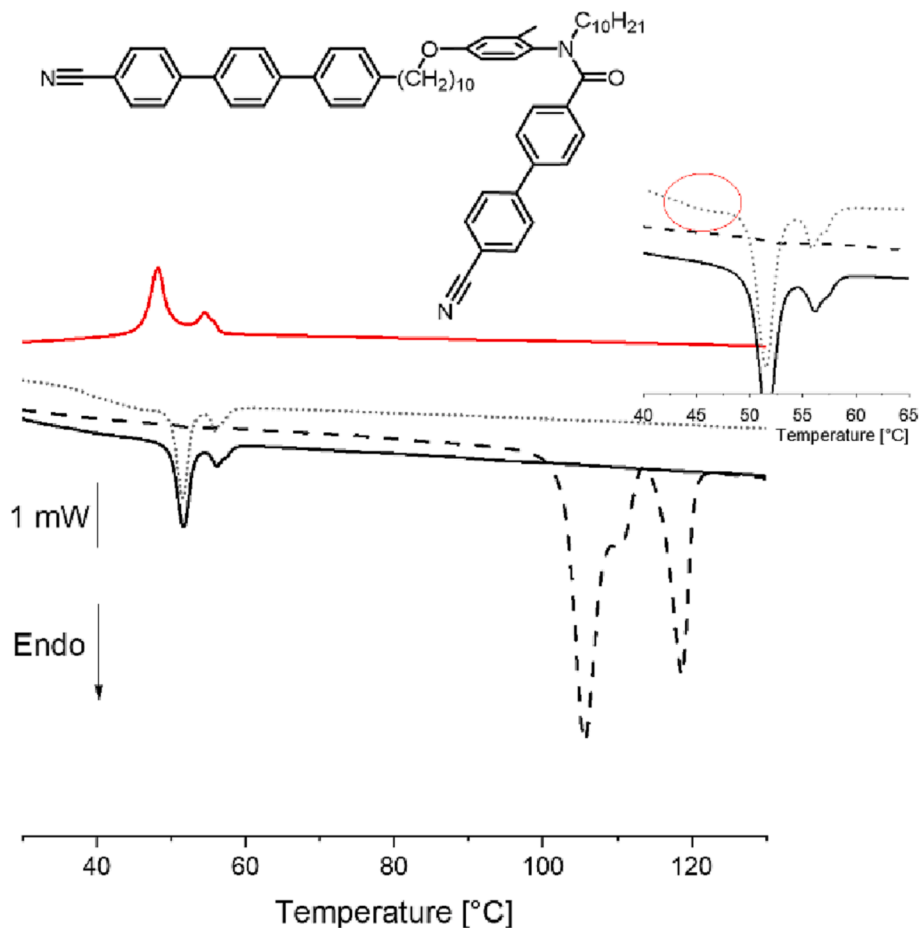


Fig. 12. The DSC traces of **4**. Dashed line is the initial heat, the red upper line the cooling trace, and the solid black line the reheat. The dotted line is the reheat after storage of the sample at RT for over a year. Inset shows the weak glass transition observed prior to the transition to the nematic phase for the aged sample. (For interpretation of the references to colour in this figure legend, the reader is referred to the web version of this article.)

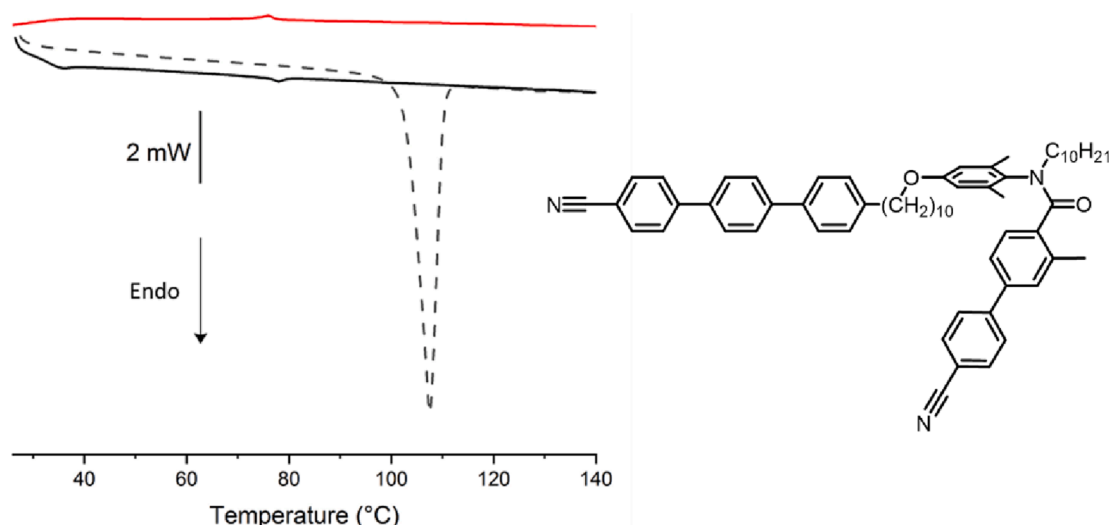


Fig. 13. The DSC trace of 8. Dashed line is the initial heat, the red line is the cooling trace and the solid black line the reheat. (For interpretation of the references to colour in this figure legend, the reader is referred to the web version of this article.)

compound 7 does form a nematic phase, and the value of T_{NI} is essentially identical to that of 4. This strongly suggests that the addition of the second methyl substituent *ortho* to the carbonyl group has no impact on molecular shape.

The tri-*ortho* substituted compound 8 melts at 108 °C directly into the isotropic phase on initial heating, and then on cooling enters the nematic phase at 76 °C. After the initial melt, it did not crystallise again, but formed a glass on cooling with a glass transition at 36 °C on heating and clears at 77 °C. The DSC traces are shown in Fig. 13. Surprisingly the value of T_{NI} for 8 having three methyl substituents is higher than those of 4, 6, and 7. Indeed it is apparent that the effects of each methyl substituent are not simply additive. The counter-intuitive increase in T_{NI} seen for 8 may be accounted for, however, by the increased proportion of the more linear *Z* amide conformer seen in this material described earlier. The more rod-like *Z* conformer will be favoured by the nematic environment, and it is probable that the proportion of *Z* conformer will be higher than that estimated in solution.

3.5. Comparing the effects of replacing an *N*-methyl substituent by an *N*-decyl chain

If we first consider the compounds with a single *ortho* methyl substituent, 4 and 5, the *N*-decyl substituent leads to a decrease in both T_m and T_{NI} compared to the corresponding *N*-methyl compounds reported previously,[4,5] and this is to be expected when increasing the size of lateral substituents in a liquid crystalline material.[15,16] The reduction in T_m is sufficient to allow enantiotropic nematic behaviour to be observed, and whereas 4 had a nematic range of just 4 °C, the nematic phase of 5 was present over an 80 °C range.

Compound 6, with two methyl substituents *ortho* to the nitrogen, did not show liquid crystalline behaviour despite the decrease in melting point compared to its *N*-methyl analogue, which was also non-mesogenic.[5] This suggests that the symmetric substitution of the anilide ring inhibits the formation of liquid crystal phases although the physical significance of this observation is not apparent.

For 7, which has two methyl substituents, one on each ring, the nematic phase was monotropic, and only present for a few degrees prior to crystallisation. T_{NI} for this compound was 57 °C, only 1 °C higher than that of 4, despite the larger proportion of the more elongated *Z* conformer expected for 7. This contrasts starkly with the nearly 50 °C increase seen when comparing the corresponding *N*-methylated compounds.[4,5] This may indicate that the presence of *ortho* methyl substituents on both sides of the amide group prevents the decyl chain from

lying along the long axis of the molecule. The loss of such conformations leads to an increase in the 'effective size' of the decyl group in 7 compared to that in compound 4 and decreases the structural anisotropy to a greater extent.

The final compound, the tri-methyl substituted 8, had the highest value of T_{NI} of the five compounds with a cyanobiphenyl terminal group. This may be attributed to the greatly increased proportion of the elongated *Z* conformer compared to 4, 6, and 7. While both T_m and T_{NI} were reduced compared to the *N*-methyl analogue, the larger *N*-decyl group tended to suppress the crystallisation of 8, and it instead formed a glass on cooling. This means that, despite the decrease in T_{NI} , the *N*-decyl substituted 8 had a nematic phase range of over 40 °C, while that of the *N*-methyl analogue was less than 10 °C.

4. Conclusions

Varying the size and nature of the *N*-substituent has a negligible effect on the conformational preferences and rotational barriers for benzanilides having a single methyl substituent *ortho* to the amide nitrogen. The introduction of larger substituents on the amide nitrogen introduces a new approach to molecular designs aimed at promoting liquid crystallinity in 3° benzanilide-based materials. The introduction of the flexible *N*-decyl substituent leads to a decrease in the melting point and suppresses crystallisation compared to the corresponding methyl-substituted materials. The increased proportion of the *Z* amide conformer caused by the introduction of methyl substituents on both benzanilide rings promotes liquid crystallinity. The combination of an *N*-decyl substituent and the inclusion of an additional phenyl ring for compound 5 leads to the formation of a wide temperature-range nematic phase. This design approach can now be exploited to obtain 3° benzanilides that exhibit a wide range of liquid crystalline behaviour.

CRediT authorship contribution statement

Grant J. Strachan: Investigation, Writing – original draft. Amerigo Zattarin: Investigation. John M.D. Storey: Supervision. Corrie T. Imrie: Supervision, Writing – review & editing.

Declaration of Competing Interest

The authors declare that they have no known competing financial interests or personal relationships that could have appeared to influence the work reported in this paper.

Data availability

Data is supplied in the [supporting information file](#).

Appendix A. Supplementary material

Supplementary data to this article can be found online at <https://doi.org/10.1016/j.molliq.2023.122160>.

References

- [1] R.A. Vora, R. Gupta, A Homologous Series containing Ester and Amide Groups as Central Linkages: 4(4'-n-Alkoxybenzoyloxy)-4"-n-Heptyloxy Benzanilides, *Mol. Cryst. Liq. Cryst.* 67 (1981) 215–220.
- [2] G. Mohiuddin, et al., Amide linkage in novel three-ring bent-core molecular assemblies: polar mesophases and importance of H-bonding, *Liq. Cryst.* 45 (2018) 1549–1566.
- [3] K. Gomola, et al., An optically uniaxial antiferroelectric smectic phase in asymmetrical bent-core compounds containing a 3-aminophenol central unit, *J. Mater. Chem.* 20 (2010) 7944.
- [4] G.J. Strachan, W.T.A. Harrison, J.M.D. Storey, C.T. Imrie, Understanding the remarkable difference in liquid crystal behaviour between secondary and tertiary amides: the synthesis and characterisation of new benzanilide-based liquid crystal dimers, *Phys. Chem. Chem. Phys.* 23 (2021) 12600–12611.
- [5] G.J. Strachan, M.M. Majewska, D. Pocięcha, J.M.D. Storey, C.T. Imrie, Using Lateral Substitution to Control Conformational Preference and Phase Behaviour of Benzanilide-based Liquid Crystal Dimers, *ChemPhysChem* 24 (2023), e202200758.
- [6] C.T. Imrie, P.A. Henderson, Liquid crystal dimers and higher oligomers: Between monomers and polymers, *Chem. Soc. Rev.* 36 (2007) 2096–2124.
- [7] M. Rickhaus, L. Jundt, M. Mayor, Determining Inversion Barriers in Atrop- isomers – A Tutorial for Organic Chemists, *Chim. Int. J. Chem.* 70 (2016) 192–202.
- [8] G.S. Attard, C.T. Imrie, Trimeric liquid crystals containing lateral alkyl chains, *Liq. Cryst.* 6 (1989) 387–390.
- [9] W. Weissflog, D. Demus, Compounds with lateral long-chain substituents — a new molecule structure concept for thermotropic liquid crystals, *Cryst. Res. Technol.* 18 (1983) K21–K24.
- [10] W. Weissflog, D. Demus, Thermotropic liquid crystalline compounds with lateral long-chain substituents (II): Synthesis and liquid crystalline properties of 1,4-Bis [4-substituted-benzoyloxy]-2-n-alkylbenzenes, *Cryst. Res. Technol.* 19 (1984) 55–64.
- [11] W. Weissflog, A. Wiegeleben, S. Haddawi, D. Demus, Thermotropic liquid crystalline compounds with lateral long chain substituents part IX linking of lateral aliphatic chains to three-ring mesogens by different functional groups, *Mol. Cryst. Liq. Cryst. Sci. Technol. Sect. Mol. Cryst. Liq. Cryst.* 281 (1996) 15–25.
- [12] C.T. Imrie, L. Taylor, The preparation and properties of low molar mass liquid crystals possessing lateral alkyl chains, *Liq. Cryst.* 6 (1989) 1–10.
- [13] E. Cruickshank, R. Walker, J.M.D. Storey, C.T. Imrie, The effect of a lateral alkyloxy chain on the ferroelectric nematic phase, *RSC Adv.* 12 (2022) 29482–29490.
- [14] M. Jasiurkowska-Delaporte, T. Rozwadowski, E. Juszyńska-Gałązka, Kinetics of Non-Isothermal and Isothermal Crystallization in a Liquid Crystal with Highly Ordered Smectic Phase as Reflected by Differential Scanning Calorimetry, Polarized Optical Microscopy and Broadband Dielectric Spectroscopy, *Crystals* 9 (2019) 205.
- [15] C.T. Imrie, Laterally substituted dimeric liquid crystals, *Liq. Cryst.* 6 (1989) 391–396.
- [16] V.S. Bezborodov, R. Dabrowskis, V.F. Petrov, V.I. Lapanik, Synthesis and properties of some laterally substituted liquid crystals, *Liq. Cryst.* 21 (1996) 801–806.